BORNEO JOURNAL OF SCIENCES AND TECHNOLOGY (BJoST)
VOL. : 6, ISSUE: 1 , 28-38
DOI: http://doi.org/10.35370/bjost.2024.6.1-04
e-ISSN: 2672-7439 © 2018, UTS Publisher.

University of Technology Sarawak

ORIGINAL ARTICLE

Behaviour of Concrete-Filled Plastic Tube (CFPT) Embedded with Reinforcement Bar under Axial Compressive Load

*Patrick Zheng-Feng Yii and Jen-Hua Ling

School of Engineering and Technology, University of Technology Sarawak, 96000 Sibu, Sarawak, Malaysia

ABSTRACT - This study developed a new concrete-filled plastic tube, known as RE CFPT for use in structural engineering applications, particularly as compression members like columns. RE CFPT was made of Unplasticized Polyvinyl Chloride (UPVC) as the external tube, concrete as the infill, and rebar as the internal reinforcement. The aim was to investigate the behaviour performance of RE CFPT under axial load. A total of 108 specimens were prepared and tested in the laboratory. 27 of which were control specimens with no rebar. The parameters studied included the tube diameter (83 mm to 160 mm), tube height (250 mm to 500 mm), and rebar size (10 mm to 16 mm). The results showed that the axial stress capacity increased as (a) the tube diameter decreased, (b) the specimen's height decreased, and (c) the rebar size increased.

ARTICLE HISTORY
Received: 9 Nov 2023
Revised: 16 Dec 2023
Accepted: 12 Jan 2024

KEYWORDS
Concrete-filled tube,
UPVC,
Reinforcement bar,
Axial load.

INTRODUCTION

Concrete-filled plastic tube (CFPT) is a composite column with a concrete core encased in a plastic tube, such as HDPE, PVC or UPVC tubes [1]. Figure 1 shows the cross-sectional of a typical CFPT design. The concrete core enhances the axial load capacity and local buckling resistance of the plastic tube [2]. The plastic tube offers lateral confinement that delays the shear cracks' propagation [3]. This allows the concrete core to undergo straining and expansion beyond the elastic stage without shear failure [4]. This subsequently enhances the column's axial load capacity [5]. Karthikeyan et al. [6] found that the confinement of HDPE, PVC and UPVC tubes increased the axial stress capacity of concrete columns by 6%, 19.43% and 39.54%.

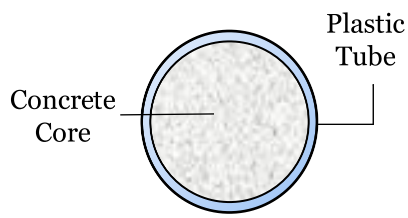

Figure 1. Cross-section of CFPT

CFPT can be applied to marine structures. The plastic tube protected the concrete core from seawater corrosion. [7]. The strength improvement given by the plastic tube showed no degradation after 6 months of submergence in seawater [8; 9]. Gupta and Verma [8] reported that the UPVC-confined concrete strength was 1.2 to 1.37 times greater than the unconfined concrete strength under marine environments.

CFPT is less common than concrete-filled steel tubes (CFST) in practice due to its inferior performance. Plastic tube has a modulus of elasticity that is approximately 1/50 that of steel tubes [10]. The confining effect of the plastic tube is less than the steel counterparts [11]. Thus, the axial load capacity of CFPT is approximately 30% of that of CFST of the same dimension [12; 13].

*Corresponding Author: Patrick Zheng-Feng Yii. University of Technology Sarawak (UTS), email: meg22030006@uts.edu.my

In recent years, researchers proposed various designs to strengthen the CFST through internal and/or external reinforcements [14-21] (Figure 2). These reinforcement methods were thought applicable to the CFPT.

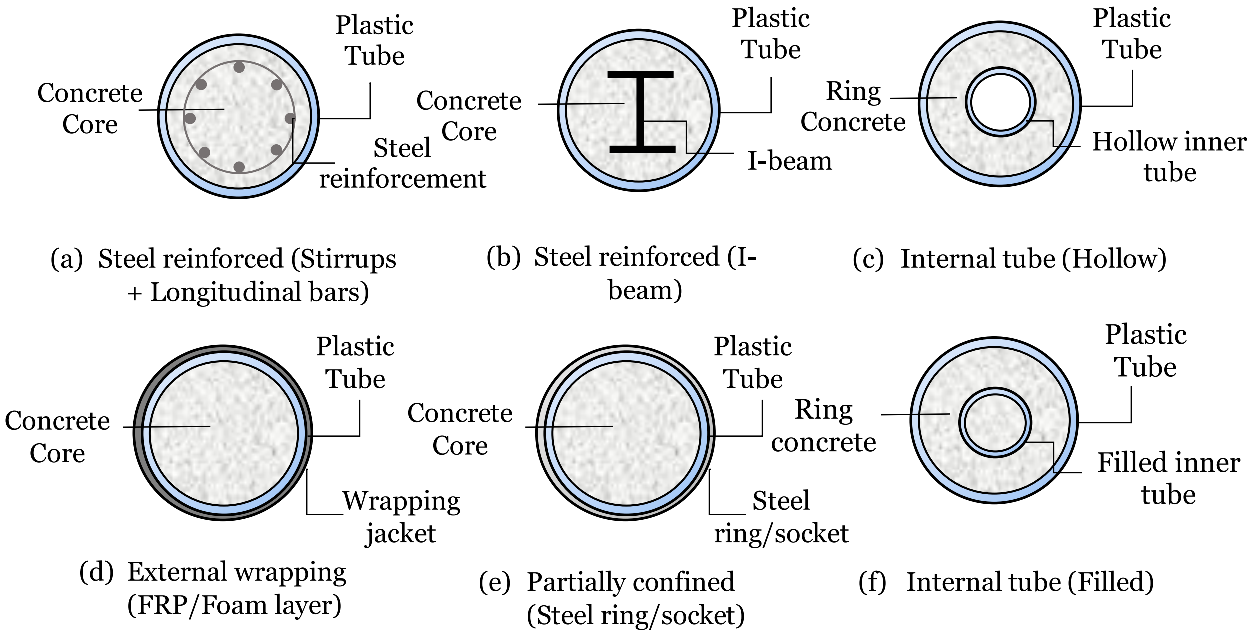

Figure 2. Designs of CFPT

Steel reinforcements and internal tubes were popularly used as internal reinforcements. They are embedded and protected by the concrete core and/or the plastic tube. This prevented their exposure to seawater corrosion [22]. Steel reinforcements are susceptible to corrosion, and thus should be applied internally. The external reinforcement should be corrosion-resistant. Otherwise, treatments and coating should be applied to the external tube to prevent corrosion.

In this study, a rebar-embedded (RE) CFPT was proposed. High-strength steel bars were embedded in CFPTs as a means to strengthen the axial stress capacity (Figure 3). A series of specimens with various diameters, heights, and rebar sizes were tested with compressive loads. The behaviour of RE CFPT under axial compressive load was investigated.

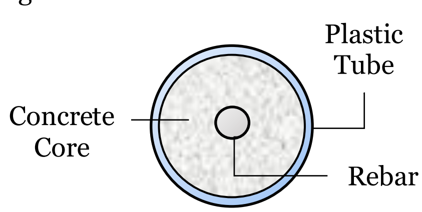

Figure 3. Rebar-embedded (RE) CFPT

EXPERIMENTAL PROGRAM

General

A total of 108 specimens were fabricated and tested with axial loads until failure. There were 27 control specimens (without rebar) and 81 RE CFPT specimens. The specimens were classified into 9 groups of different diameters and heights, ranging from 83 mm to 160 mm and 250 mm to 500 mm, respectively. The specifications of the specimens are tabulated in Table 1.

Table 1. Specifications of the Specimens

Group	Specimens[*1]	Specifications			
		Diameter, d (mm)	Height, h (mm)	Thickness, t (mm)	Rebar size, d_r (mm)
G1	C83-250-0 R83-250-10 R83-250-12 R83-250-16	83	250	2	0 10 12 16
G2	C83-375-0 R83-375-10 R83-375-12 R83-375-16	83	375	2	0 10 12 16
G3	C83-500-0 R83-500-10 R83-500-12 R83-500-16	83	500	2	0 10 12 16
G4	C111-250-0 R111-250-10 R111-250-12 R111-250-16	111	250	2	0 10 12 16
G5	C111-375-0 R111-375-10 R111-375-12 R111-375-16	111	375	2	0 10 12 16
G6	C111-500-0 R111-500-10 R111-500-12 R111-500-16	111	500	2	0 10 12 16
G7	C160-250-0 R160-250-10 R160-250-12 R160-250-16	160	250	2	0 10 12 16
G8	C160-375-0 R160-375-10 R160-375-12 R160-375-16	160	375	2	0 10 12 16
G9	C160-500-0 R160-500-10 R160-500-12 R160-500-16	160	500	2	0 10 12 16

Notes:
[*1] C defines as control specimens that without rebar (d_r = 0); R defines as rebar embedded specimens.

Material Properties

PVC tubes

UPVC tubes with various diameters (83 mm, 111 mm and 160 mm) and heights (250 mm, 375 mm and 500 mm) were used as the external tube. The tube diameters and heights were chosen based on the specifications of the Universal Testing Machine (for axial test of CFPT) which are the maximum size of compression plates (240 mm × 240 mm) and the space for compression test (150 to 1000 mm). To determine the mechanical properties of the UPVC tube material, three tensile coupons were prepared and tested using a Universal Tensile Machine (UTM) based on ASTM D638 [23]. Figures 4 and 5 show the UTM and the experiment setup respectively. Figure 6 displays the dimension of the UPVC tensile coupon.

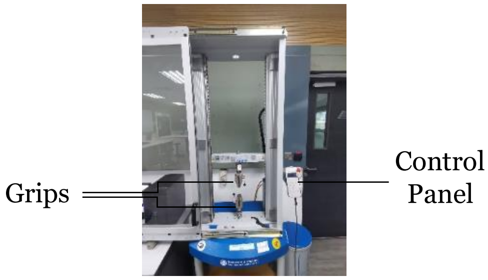

Figure 4. Universal Tensile Machine

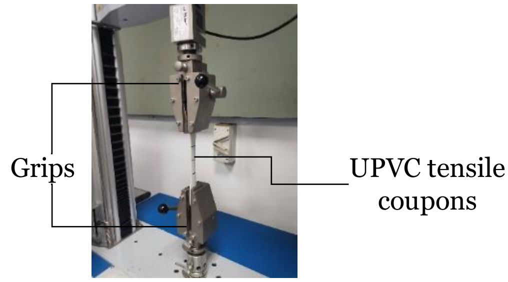

Figure 5. Tensile test of UPVC Tensile Coupon

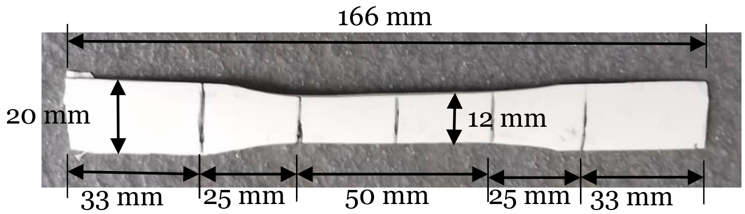

Figure 6. Dimension of UPVC Tensile Coupon

The ultimate tensile stress was obtained from the test results and recorded in Table 2. The UPVC tubes used in this study were considered acceptable as they achieved their ultimate tensile strength of 25 MPa according to standard ISO 1452-2 [24].

Table 2. Mechanical Properties of UPVC Tube Material

Mechanical Properties	Sample 1	Sample 2	Sample 3	Average
Ultimate tensile strength (MPa)	38.12	38.50	43.24	39.95

Concrete

The UPVC tubes were filled with Grade 20 ready-mixed concrete. To determine the workability of the concrete, a slump test was performed (Figure 7). The slump was 116 mm, which is considered high workability according to ASTM C143 [25].

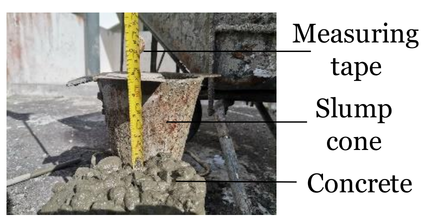

Figure 7. Slump Test

Eighteen (18) concrete cubes of 150 mm size were prepared to determine the density and strength of concrete on day 28 (Figure 8). Two (2) concrete cubes were tested under compressive load using a compressive machine, and the average compressive strength was taken.

Figure 8. Concrete Cube Test

The concrete cube test results were tabulated in Table 3. From Table 3, the concrete strength was considered acceptable as it reached its required strength at maturity according to BS EN 12390-3 [26].

Table 3. Concrete Cube Test Results

Specimens group	Density (kg/m^3)			Concrete cube strength at 28th days (MPa)		
	Sample 1	Sample 2	Average	Sample 1	Sample 2	Average
G1 G2	2359	2356	2358	19.5	19.8	19.7
G3 G4	2373	2350	2362	19.4	20.6	20.0
G5 G6	2364	2409	2387	19.5	21.7	20.6
G7	2382	2427	2405	22.9	21.9	22.4
G8	2314	2370	2342	20.4	22.5	21.5
G9	2361	2376	2369	19.9	21.0	20.5

High-tensile steel reinforcement bars (Rebars)

The rebars used were high-tensile steel bars with various diameters (10 mm, 12 mm and 16 mm). The rebar sizes were chosen to provide sufficient spacing to the CFPT to achieve adequate concrete consolidation. To determine the mechanical properties of the steel rebar, three rebars for each diameter were prepared and tested with tensile load using a Universal Testing Machine (Figure 9), based on the standard ASTM-A615 [27].

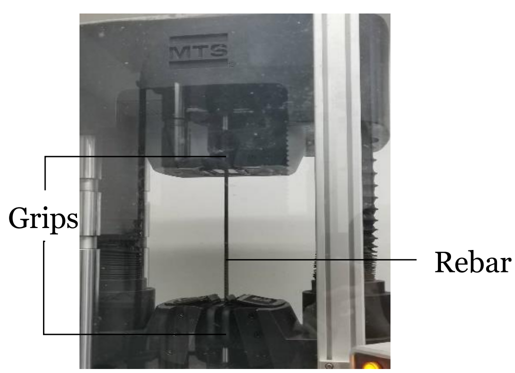

Figure 9. Tensile Test of Rebar

Table 4 tabulates the testing results of the rebars. The steel rebars were considered acceptable as they achieved their nominal tensile strength of 500 N/mm2.

Table 4. Mechanical Properties of Steel Reinforcement Bars

Rebar size (mm)	Ultimate tensile strength (MPa)			
	Sample 1	Sample 2	Sample 3	Average
10	643	701	666	670
12	683	649	681	671
16	622	648	640	637

Testing Procedures

The CFPT specimens were tested under increasing axial compressive load using a 2000 kN Universal Testing Machine at the Heavy Structure Lab at the University of Technology Sarawak. Two pieces of gypsum boards (9mm thickness) were placed at the top and the bottom of the specimens to avoid the concentration of stress on the contact surface of the specimens that could fail the specimen prematurely. The load was applied to the specimens by lowering the top plate until the failure. Figure 10 shows the setup of the axial load test.

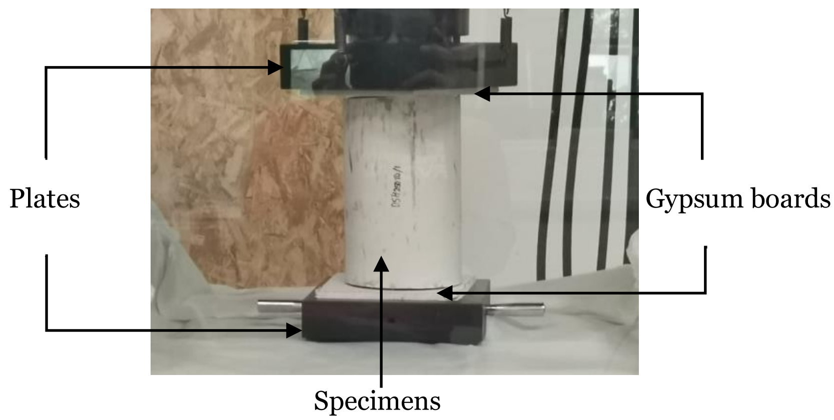

Figure 10. Setup of Axial Load Test

The axial load capacity, P_u of the specimens was obtained from the test results. The effects of the tube diameters, tube heights and rebar sizes on the axial load capacity, P_u and axial stress capacity, f_u were investigated.

Results

Table 5 tabulates the axial load capacity of the specimen, P_u. Three specimens were tested. The axial load capacity was taken. The axial stress capacity, f_u was computed using P_u (Eq. 1). The load was assumed equally distributed across the area, regardless of the materials.

$$f_u = P_u/A \quad \text{(Eq. 1)}$$

Table 5. Ultimate axial capacity and axial stress capacity of CFPT specimens

Group	Area, *A* (mm^2)	Specimens	Axial load capacity, P_u (kN)				Failure Mode	Axial stress capacity, f_u (MPa)
			1	2	3	Average		
1	5410.6	C83-250-0	114.9	126.6	116.6	119.4	Drum	22.1
		R83-250-10	133.2	133.1	123.6	130.0	Drum	24.0
		R83-250-12	147.6	136.0	148.6	144.1	Drum	26.6
		R83-250-16	196.9	200.5	197.7	198.8	Drum	36.7
2		C83-375-0	103.5	109.6	95.7	102.9	Drum	19.0
		R83-375-10	120.3	98.2	98.8	105.8	Buckling	19.5
		R83-375-12	123.0	132.7	106.7	120.8	Buckling	22.3
		R83-375-16	172.2	178.5	145.5	165.4	Buckling	22.1
3		C83-500-0	83.0	105.5	111.1	99.9	Drum	18.5
		R83-500-10	135.1	116.8	118.9	123.6	Buckling	22.8
		R83-500-12	110.7	101.6	113.9	108.7	Buckling	20.1
		R83-500-16	136.5	138.7	147.0	140.7	Buckling	26.0
4	9676.9	C111-250-0	250.1	214.1	200.3	221.5	Drum	22.9
		R111-250-10	230.1	222.0	216.6	222.9	Shear	23.0
		R111-250-12	217.7	203.3	255.2	225.4	Shear	23.3
		R111-250-16	264.1	237.3	254.9	252.1	Drum	26.1
5		C111-375-0	186.7	209.3	213.4	203.1	Drum	21.0
		R111-375-10	217.3	185.7	173.7	192.2	Shear	19.9
		R111-375-12	226.4	216.6	223.7	222.2	Shear	23.0
		R111-375-16	241.0	221.8	256.1	240.3	Drum	24.8
6		C111-500-0	129.1	135.6	118.1	129.1	Drum	13.2
		R111-500-10	172.8	157.6	145.7	158.7	Drum	16.4
		R111-500-12	150.8	156.9	167.9	158.6	Buckling	16.4
		R111-500-16	170.9	182.5	226.0	193.1	Buckling	20.0
7	20106.2	C160-250-0	428.9	470.0	502.6	467.2	Drum	23.2
		R160-250-10	396.6	435.4	428.2	420.1	Drum	20.9
		R160-250-12	497.7	521.6	493.1	504.1	Drum	25.1
		R160-250-16	474.5	481.0	490.0	481.8	Drum	24.0
8		C160-375-0	492.7	431.8	412.0	445.5	Drum	22.2
		R160-375-10	451.7	431.0	465.0	449.2	Drum	22.3
		R160-375-12	463.7	431.3	430.8	441.9	Drum	22.0
		R160-375-16	471.2	454.6	462.1	462.6	Drum	23.0
9		C160-500-0	396.2	388.6	399.2	394.7	Drum	19.6
		R160-500-10	379.6	353.2	359.5	364.1	Drum	18.1
		R160-500-12	374.7	382.9	405.8	387.8	Drum	19.3
		R160-500-16	368.7	380.7	318.5	356.0	Drum	17.7

DISCUSSION

Failure Modes

The failure modes for the specimens observed were drum, shear and buckling failures (Figure 11). Drum failure was found in all control specimens and some RE CFPT specimens from groups 1, 4, 5, 6, 7, 8 and 9. These specimens were either with no rebar, short (h = 250 mm) or with moderate to large diameter, d = 111 and 160 mm). This failure was mainly due to the (a) internal crushing of concrete, and (b) excessive lateral expansion of the concrete core under compressive load [3]. The internal stress caused by the concrete crushing and expansion exceeded the confinement stress given by the plastic tube. Hence, the plastic tube dilated and the specimen failed.

Shear failure was found in the RE CFPT specimens from groups 4 and 5. These specimens were either with moderate tube diameter (d = 111 mm), short to moderate height (h = 250 and 375 mm), or embedded with rebars of small to moderate sizes (d_r = 10 and 12 mm). This failure happened when the shear stress exceeded the concrete strength due to the shear crack propagation. RE CFPT specimens should be more resilient to shear failure, in theory. The shear crack propagation was believed to be, to some degree, restricted by (a) the axial resistance provided by the rebar and (b) the confining stress offered by the plastic tube [4]. However, the specimens were found to fail shear. The actual cause of this failure in the RE CFPT specimens would require further study.

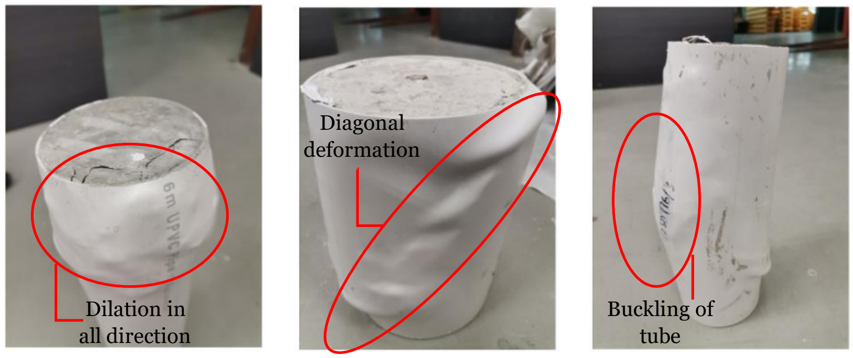

(a) Drum failure (b) Shear failure (c) Buckling failure

Figure 11. Failure Modes

Buckling failure was found in the RE CFPT specimens from groups 2, 3 and 6. These specimens were either with small to moderate tube diameters (d = 83 and 111 mm) or with moderate to tall tube heights (h = 375 and 500 mm). This failure might be due to the horizontal stress generated during the rebar buckling [28]. As the tube height increased, the embedded rebar was slenderer and more susceptible to buckle. The buckling response of the rebar generated lateral stress, causing the RE CFPT to deform sideways (Figure 12).

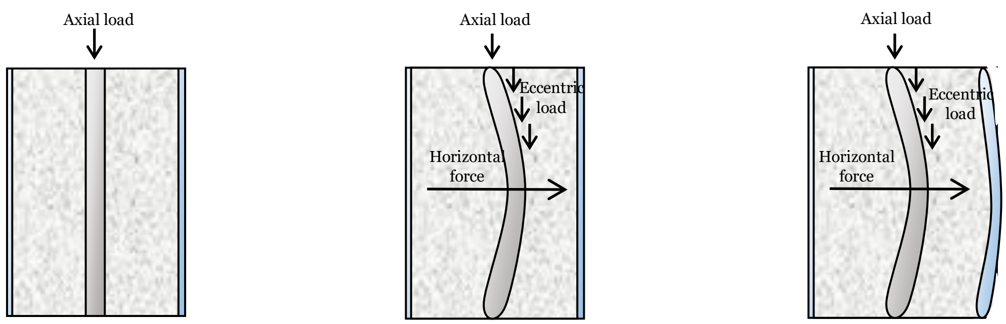

(a) (b) (c)

Figure 12. Buckling Failure

Effect of Tube Diameter

Comparing the RE CFPT specimens from groups 1 and 7, groups 2 and 8, and groups 3 and 9, the diameter increased from 83 mm to 160 mm. The axial load capacity increased by 2.43 to 4.25 times, while the axial stress capacity, f_u of the RE CFPT specimens decreased by 1% to 35%.

As the diameter increased from 83 mm to 160 mm, the area of the specimens increased by 3.72 times. This led to the increment of the axial load capacity. However, as the diameter increased, the thickness-to-diameter ratio, $2t/d$ decreased. The effective confining pressure provided by the tube decreased [29]. Thus, the axial stress capacity, f_u of the specimen decreased.

Effect of Tube Height

Comparing the specimens from groups 1 and 3, groups 4 and 6, and groups 7 and 9, as the height increased from 250 mm to 500mm, the axial stress capacity, f_u were decreased by 5% to 42.36%. As the tube height increased, the buckling critical load decreased, and the specimen and the embedded rebar were more susceptible to buckling [3, 28].

Effect of Rebar Size

Comparing the axial stress capacity, f_u of the control and RE CFPT specimens from groups 1 to 6, the rebar size increased from 10 mm to 16 mm, and the axial stress capacity, f_u increased by 14.0% to 52.9%. The rebar area increased with the rebar size, and the axial resistance provided by the rebar therefore increased. Besides, as the rebar size increased, the slenderness ratio of the rebar decreased. This increased the buckling critical load and caused the rebar to be less susceptible to buckling [28].

For the specimens with the largest diameter of 160 mm (Groups 7 to 9), the axial stress capacity, f_u no longer increased as the rebar size increased. For the specimens with large diameters (160 mm), the ratio of the rebar area to the specimen area was relatively low ($A_r/A \leq$ 1.0%). Assuming the axial load was evenly distributed over the specimen area regardless of the material, the axial load was mostly supported by the concrete instead of the rebar. Thus, the axial capacity provided by the rebar was insignificant (-1.5% to 8.2%).

CONCLUSION

Based on the results of the experimental study, it was concluded that:

i) The rebar increases the axial stress capacity of the CFPT due to its high axial resistance. The axial stress capacity of the CFPT was increased by a maximum of 66% when 16 mm-sized rebar was embedded in the CFPT in group 1 (d = 83 mm, h = 250 mm). However, the performance of rebar in enhancing the CFPT's axial resistance in the marine environment remains unclear. This requires further research in the future.

ii) Drum failure was more likely to occur for the RE CFPT specimens, especially for the specimens with large diameters (d = 160 mm). Buckling failure was most likely to occur when the rebar slenderness ratio, h/d was higher than 20.83. Shear failure rarely occurred in the RE CFPT specimens. It required further studies to investigate the conditions to trigger the shear failure of the RE CFPT.

iii) As the diameter of the RE CFPT increased from 83 mm to 160mm, the axial load capacity increased by 2.43 to 4.25 times while the axial stress capacity decreased by 1% to 35%. The axial load capacity increased with the diameter because of the increment of the load-carrying area. The axial stress capacity decreased with the diameter because of the reduction of the thickness-to-diameter, $2t/d$ ratio and led to the weakening of the tube confining stress.

iv) As the height of the RE CFPT increased from 250 mm to 500mm, the axial stress capacity decreased by 5% to 42.36%. The embedded rebar length increased with the specimen's height. Thus, as the height increased, the specimens and the rebar were more susceptible to buckling failure.

v) The axial stress capacity of the RE CFPT increased by 14.0% to 52.9% when the rebar size increased from 10 mm to 16 mm. As the rebar size increased, the axial resistance provided by the rebar increased due to a larger load-carrying area. However, the axial stress capacity improvement provided to the large-diameter (160 mm) RE CFPT becomes insignificant because the axial load was mostly supported by the concrete instead of the rebar.

vi) For an optimum design of a RE CFPT, the proportion of the rebar area was recommended to exceed 1.0% of the area of the RE CFPT. This allowed the rebar to offer significant axial load capacity improvement to the CFPT. This could be achieved by either reducing the tube diameter or increasing the rebar size. Besides, the RE CFPT design was recommended to minimize the impact of rebar buckling response. The lateral stress generated by the rebar buckling response reduced the axial stress capacity of the RE CFPT. This could be solved by reducing the RE CFPT height or increasing the rebar size to prevent the rebar buckling.

ACKNOWLEDGEMENT

This study was supported by the Research Grants of the University of Technology Sarawak, UTS/RESEARCH/2/2022/15.

REFERENCES

[1] N.A. Abdulla, "Concrete Encased with Engineering Plastics", *Journal of Civil Engineering and Construction*, vol. 9, no. 1, pp 31-41, 2020, doi: 10.32732/jcec.2020.9.1.31.

[2] W.O. Oyawa, N.K. Gathimba, and G.N. Mang'uriu, "Structural response of composite concrete filled plastic tubes in compression", *Steel and Composite Structures*, vol. 21, no. 3, pp 589-604, 2016, doi: 10.12989/scs.2016.21.3.589.

[3] A.M. Woldemariam *et al*., "Experimental studies on the behavior of concrete-filled uPVC tubular columns under axial compression loads", *Cogent Engineering*, vol. 7, no. 1, 2020, doi: 10.1080/23311916.2020.1768649.

[4] J.H. Ling *et al.,* "Concrete-Filled Tubular Column Made of Various Types of Material: A Review", *Journal of Civil Engineering*, vol. 38, no. 1, pp 3-15, 2023.

[5] A.S. Saadoon and N.A. Jasim, "Experimental Investigation of Plain Concrete-Filled Plastic Tubular Columns", *International Journal of Advanced Research in Science, Engineering and Technology*, vol. 6, no. 3, pp 8249-8258, 2019, ISSN: 2350- 0328

[6] N. Karthikeyan *et al*., "Assessment of Concrete Cylinders Confined with HDPE, PVC & UPVC Tubes", *International Journal of Scientific & Engineering Research*, vol. 9, no. 4, pp 83-87, 2018, ISSN: 2229-5518.

[7] A. Bandyopadhyay, Y.M. Chanu, and A.K. Samanta, "Experimental Investigation on Mechanical Properties of PCC and FRC confined with UPVC Pipe" *Indian Journal of Engineering & Materials Sciences*, vol. 26 pp 342-248, 2019.

[8] P.K. Gupta and V.K. Verma, "Study of concrete-filled unplasticized poly-vinyl chloride tubes in marine environment", *Proceedings of the Institution of Mechanical Engineers, Part M: Journal of Engineering for the Maritime Environment*, vol. 230, no. 2, pp 229-240, 2016, doi: 10.1177/1475090214560448.

[9] Y.L. Li, X.L. Zhao, and R.K. Singh Raman, "Behaviour of seawater and sea sand concrete filled FRP square hollow sections". *Thin-Walled Structures*, vol. 148, 2020, doi: 10.1016/j.tws.2019.106596

[10] M. Fakharifar and G. Chen, "Compressive behavior of FRP-confined concrete-filled PVC tubular columns", *Composite Structures*, 2016, pp 91-109, doi: 10.1016/j.compstruct.2016.01.004.

[11] S. Mohammad Askari *et al*., "Performance of polypropylene fiber reinforced concrete-filled UPVC tube columns under axial compression", *Construction and Building Materials*, col. 231, 2020, doi: 10.1016/j.conbuildmat.2019.117049.

[12] P.K. Gupta, "Confinement of Concrete Columns with Unplasticized Poly-vinyl Chloride Tubes", *International Journal of Advanced Structural Engineering*, vol. 5, no. 19, 2013, doi: 10.1186/2008-6695-5-19.

[13] Z.W. Yu., F.X. Ding and C.S. Cai, "Experimental behavior of circular concrete-filled steel tube stub columns"., *Journal of Constructional Steel Research*, vol. 63, no. 2, pp 165-174, 2007, doi: 10.1016/j.jcsr.2006.03.009.

[14] A. Bandyopadhyay, A.K. Samanta and K. Michel Paul, "Assessment of Axial Capacity of RC Stub Column Confined with Unplasticized Polyvinyl Chloride Pipe", *Journal of The Institution of Engineers (India): Series A*, vol. 100, no. 4, pp 535-546, 2019, doi: 10.1007/s40030-019-00397-5.

[15] A.M. Woldemariam, W.O. Oyawa and T. Nyomboi, "Behavior of Concrete-Filled Single and Double-Skin uPVC Tubular Columns Under Axial Compression Loads", *The Open Construction and Building Technology Journal*, vol. 13, no. 1, pp 164-177, 2019, doi: 10.2174/1874836801913010164.

[16] R. Sasikanth, M. Soundar Rajan, "Experimental Investigation of Concrete Filled PVC Tube Columns Confined by Plain PVC Socket", *IT in Industry*, vol. 9, no. 3, pp 217-222, 2021, ISSN: 2203-1731.

[17] W. Xie *et al.*, "Research on I steel reinforced concrete-filled GFRP tubular short columns.", *Thin-Walled Structures*, vol. 120, pp 282-296, 2017, doi: 10.1016/j.tws.2017.08.031.

[18] T. Ozbakkaloglu and Y. Idris, "Seismic Behavior of FRP-High-Strength Concrete–Steel Double-Skin Tubular Columns", *Journal of Structural Engineering*, vol. 140, no. 6, 2014.

[19] T. Vincent and T. Ozbakkaloglu, "Influence of concrete strength and confinement method on axial compressive behavior of FRP confined high- and ultra high-strength concrete", *Composites Part B: Engineering*, vol. 50, pp 413-428, 2013, doi: 10.1016/j.compositesb.2013.02.017.

[20] F. Alatshan, *et al.*, "Explicit Simulation of Circular CFST Stub Columns with External Steel Confinement under Axial Compression", *Materials (Basel)*, vol. 13, 2020, doi:10.3390/ma13010023.

[21] S.K. Alrebeh and T. Ekmekyapar, "Structural behavior of concrete-filled steel tube short columns stiffened by external and internal continuous spirals", *Structures*, vol. 22, pp 98-108, 2019, doi: 10.1016/j.istruc.2019.07.001.

[22] R. Kumutha and K. Vijai, "External Confinement of Plain and Reinforced Concrete Columns using PVC Pipes", *2nd International Conference on Structural Architectural and Civil Engineering*, 2016, Dubai, ISBN: 9788193137376.

[23] ASTM International, *ASTM D638 Standard Test Method for Tensile Properties of Plastics*., ASTM: West Conshohocken PA, USA, 2014.

[24] International Standard, *ISO 1452-2 Plastics piping systems for water supply and for buried and above-ground drainage and sewerage under pressure — Unplasticized poly(vinyl chloride) (PVC-U) — Part 2: Pipes*. 2009.

[25] ASTM International, *ASTM C143/C143M-20 Standard Test Method for Slump of Hydraulic-Cement Concrete*., ASTM: West Conshohocken PA, USA, 2020.

[26] British Standard Instituition, *BS-EN 12390-3 Testing Hardened Concrete Part 3: Compressive Strength of Test Specimens*., London, British Standard Instituition (BSI), 2002

[27] ASTM International, *ASTM A615/A615M - 12 Standard Specification for Deformed and Plain Carbon-Steel Bars for Concrete Reinforcement*., ASTM: West Conshohocken PA, USA, 2012.

[28] H. Yang, P.X. Sun and Y.J. Deng, "Experiment Investigation of the Influence of Reinforcing Bar Buckling on Seismic Behavior of RC Columns", *Engineering Structures*, vol. 220, pp 1-19, 2020, doi: 10.1016/j.engstruct.2020.110923.

[29] A.M. Woldemariam, W.O. Oyawa and T. Nyomboi, "Structural Performance of UPVC Confined Concrete Equivalent Cylinders Under Axial Compression Loads", *Buildings*, vol. 82, pp 1-25, 2019, doi: 10.3390/buildings9040082.